

# A Novel Nested Array Design for Direction of Arrival Estimation of Noncircular Signals

Weijian Si, Zhanli Peng, Changbo Hou<sup>\*</sup>, and Fuhong Zeng

**Abstract**—In this paper, a novel nested array is proposed for direction of arrival (DOA) estimation of noncircular signals. By using the noncircular property, we can get a virtual array composed of difference coarray (DCA) and sum coarray (SCA). Specifically, we give the properties of DCA and SCA for the generalized translational nested array first. Then, based on the relationship between DCA and SCA, an optimal translational nested array with increased degrees of freedom (DOFs) is constructed. To extend the physical array aperture, we move part of sensors in the translational nested array to the mirrored locations. Accordingly, the novel nested array with increased DOFs and physical array aperture is obtained. Finally, superiority of the proposed array is demonstrated by simulation experiments.

## 1. INTRODUCTION

Sparse arrays have attracted considerable attention from researchers in recent years due to their large inter-element spacing and underdetermined direction of arrival (DOA) estimation ability [1–5]. Typical sparse arrays, such as minimum redundancy arrays (MRAs) [6], nested arrays (NAs) [1], and coprime arrays (CPAs) [7], can resolve  $O(N^2)$  sources with  $O(N)$  physical sensors. Accordingly, many modified versions [8–10] of the above sparse arrays have been presented, where their virtual arrays consist only of difference coarray (DCA), i.e., only the property of circular signals is considered.

However, in practical applications, lots of noncircular signals also exist, e.g., binary phase shift keying (BPSK), pulse amplitude modulation (PAM), and minimum shift keying (MSK), etc.. Research results in [11] indicate that the ellipse covariance matrix of noncircular signals is not equal to zero, which means that they can be exploited for DOA estimation combined with the covariance matrix. Thus, based on this property, many DOA estimation methods for noncircular signals were proposed, such as noncircular Root-MUSIC [11], noncircular ESPRIT [12], and MUSIC-Like method [13], etc. However, the above methods can only be used in uniform linear arrays (ULAs) for DOA estimation, which indicates that only  $2(N - 1)$  noncircular signals can be detected with  $N$  physical sensors.

Recently, some DOA estimation methods about noncircular signals based on sparse arrays have been proposed to improve the DOA estimation performance. In [14], the researchers presented an ambiguity-free DOA estimation method for unfold CPA. By using the coprime property of unfold CPA, the ambiguity problem is suppressed effectively. Nevertheless, only at most  $2(M + N - 1)$  noncircular signals can be detected when a unfold CPA with  $M + N - 1$  physical sensors is used. Since the noncircular signals possess non-zero ellipse covariance matrix, it can be vectorized to generate the sum coarray (SCA) [15–17]. Therefore, based on this, some subspace-based [15, 17] and compressive sensing-based [16, 18] underdetermined DOA estimation methods for noncircular signals have also been proposed. Through the joint use of DCA and SCA, the number of continuous virtual sensors extended by these sparse arrays can be increased dramatically, which can further contribute to the improvement of DOA estimation performance. For convenience, we name the number of continuous virtual sensors as

---

Received 4 October 2019, Accepted 23 November 2019, Scheduled 9 December 2019

<sup>\*</sup> Corresponding author: Changbo Hou (houchangbo@hrbeu.edu.cn).

The authors are with the College of Information and Communication Engineering, Harbin Engineering University, Harbin, China.

continuous degrees of freedom (cDOFs). Note that, the above DOA estimation methods are proposed based on the prototype NA and CPA, whose physical structures are not optimal for the DOA estimation of noncircular signals.

To achieve the underdetermined DOA estimation of noncircular signals with increased cDOFs, diff-sum coprime array with multiperiod subarrays (DsCAMpS) is proposed in [17]. By complementing DCA with SCA, the cDOFs of DsCAMpS is increased compared to that of traditional CPA. However, high redundancy between DCA and SCA indicates that DsCAMpS is not optimal. Thus, some new sparse array design strategies inspired by nested concept have been presented. In [15], a new nested array (NNA) with sum and difference composite coarray (SDCA) is introduced, which owns larger cDOFs than prototype NA. Unfortunately, we cannot get such NNA when the total sensor number is odd. To overcome this drawback, a nested array with displaced subarray (NADiS) is designed in [19]. By redefining the distance between dense subarray and sparse one, and expanding the inter-element spacing of sparse subarray in the prototype NA, NADiS owns significantly increased cDOFs and physical array aperture. In [20], exhaustion method is utilized to determine the optimal sparse array configuration for noncircular signals (SANC). Although SANC has achieved the maximum cDOFs, it does not possess explicit closed-form expression. What is more, some holes exist in the SDCAs of the above sparse arrays, which will restrict the DOA estimation performance for noncircular signals.

In this paper, we propose a novel nested array for DOA estimation of noncircular signals. This novel configuration not only possesses the same advantage as prototype NA, i.e., continuous virtual array, but also owns almost twice more cDOFs than the latter [1]. In addition, the physical aperture of the proposed array is also increased, which can improve the DOA estimation performance further. To obtain this novel nested array, we first give the generalized definition of translation nested array (TNA) [21]. Its corresponding properties of DCA and SCA are also introduced. Then, based on the relationship between DCA and SCA, we can determine the optimal translation distances for TNA to maximize the obtaining cDOFs. By flipping part of sensors in the optimal TNA to the negative axis, we can get the proposed array, which owns a much larger physical aperture than the optimal TNA. In the end, the DOA estimation performance of the proposed array is evaluated through simulation experiments.

The remainder of this paper is organized as follows. Section 2 reviews the system model for DOA estimation of noncircular signals. Section 3 introduces the proposed novel nested array. Simulation experiments are provided in Section 4. Section 5 concludes this paper.

## 2. SYSTEM MODEL

For an  $N$ -sensor TNA, the sensor position sets of its subarray 1 and subarray 2 can be respectively denoted as

$$\begin{cases} \mathbb{P}_1 = \{(p_1 + a_1)d | a_1 \in \mathbb{Z}, p_1 = 1, \dots, N_1\} \\ \mathbb{P}_2 = \{(p_2(N_1 + 1) + a_2)d | a_2 \in \mathbb{Z}, p_2 = 1, \dots, N_2\} \end{cases} \quad (1)$$

where  $\mathbb{Z}$  is the integer set.  $a_1d$  and  $a_2d$  represent the translation distances for subarray 1 and subarray 2, respectively.  $N_1$  and  $N_2$  are the corresponding sensor numbers, where  $N_1 + N_2 = N$ . Without loss of generality, the unit inter-element spacing  $d$  is fixed as half a wavelength. Obviously, the prototype NA is a special case of TNA with  $a_1 = a_2 = 0$ .

Assume  $K$  uncorrelated far-field narrowband noncircular signals impinge on the  $N$ -sensor TNA, where the DOA of the  $k$ th signal is  $\theta_k \in [-\pi/2, \pi/2)$ . Then, the array output at the  $t$ th snapshot can be expressed as

$$\mathbf{x}(t) = \sum_{k=1}^K \mathbf{a}(\theta_k) s_k(t) + \mathbf{n}(t) \quad (2)$$

where  $\mathbf{a}(\theta_k) = [e^{j2\pi l_1 \sin \theta_k / \lambda}, \dots, e^{j2\pi l_N \sin \theta_k / \lambda}]^T$  denotes the steering vector of the  $k$ th signal, and  $[\cdot]^T$  represents the transpose operation.  $[l_1, \dots, l_N]$  is the sensor position set, which satisfies  $l_n \in \mathbb{P}_1 \cup \mathbb{P}_2$ ,  $n = 1, \dots, N$ .  $s_k(t)$  represents the  $k$ th noncircular signal at the  $t$ th snapshot, and  $\mathbf{n}(t)$  is the additive Gaussian white noise vector. It is obvious from the noncircularity of  $s_k(t)$  that  $E[s_k(t)s_k(t)] = \rho_k e^{j\psi_k} E[s_k(t)s_k^*(t)]$  holds, where  $\psi_k$  represents the noncircular phase of  $s_k(t)$ , and

$\rho_k \in (0, 1]$  denotes the corresponding noncircular rate.  $E[s_k(t)s_k^*(t)] = \sigma_k^2$  is the  $k$ th signal power, and  $E[\cdot]$  is the expectation operation. Besides, the signal and noise are assumed to be statistically independent.

Then, the covariance matrix of  $\mathbf{x}(t)$  can be denoted as

$$\mathbf{R}_x = E[\mathbf{x}(t)\mathbf{x}^H(t)] = \mathbf{A}\mathbf{R}_s\mathbf{A}^H + \sigma_n^2\mathbf{I} \quad (3)$$

where  $\mathbf{A} = [\mathbf{a}(\theta_1), \dots, \mathbf{a}(\theta_K)]$  is the manifold matrix.  $\mathbf{R}_s = \text{diag}[\sigma_1^2, \dots, \sigma_K^2]$  is the signal covariance matrix.  $\sigma_n^2\mathbf{I}$  and  $\mathbf{I}$  respectively denote the noise covariance matrix and the  $N$ -dimensional identity matrix. The symbol  $(\cdot)^H$  denotes the conjugate transpose operation. For convenience of analysis, noncircular phases and rates for all signals are assumed to be zero and one, respectively. Under this condition, the ellipse covariance matrix of  $\mathbf{x}(t)$  and its conjugate can be respectively given as

$$\mathbf{\Gamma}_x = E[\mathbf{x}(t)\mathbf{x}^T(t)] = \mathbf{A}\mathbf{R}_s\mathbf{A}^T \quad (4)$$

$$\mathbf{\Gamma}_x^* = E[\mathbf{x}^*(t)\mathbf{x}^H(t)] = \mathbf{A}^*\mathbf{R}_s\mathbf{A}^H \quad (5)$$

In practice,  $\mathbf{R}_x$ ,  $\mathbf{\Gamma}_x$ , and  $\mathbf{\Gamma}_x^*$  are estimated by the maximum likelihood method, where the array output data with  $T$  snapshots is used. Combining Eqs. (3), (4), and (5), we can get the following expression

$$\mathbf{R} = \begin{bmatrix} \mathbf{R}_x \\ \mathbf{\Gamma}_x \\ \mathbf{\Gamma}_x^* \end{bmatrix} = \begin{bmatrix} \mathbf{A}\mathbf{R}_s\mathbf{A}^H \\ \mathbf{A}\mathbf{R}_s\mathbf{A}^T \\ \mathbf{A}^*\mathbf{R}_s\mathbf{A}^H \end{bmatrix} + \begin{bmatrix} \sigma_n^2\mathbf{I} \\ \mathbf{0} \\ \mathbf{0} \end{bmatrix} \quad (6)$$

where  $\mathbf{0}$  denotes the  $N \times N$  zero matrix.

Vectorizing Eq. (6), we have

$$\mathbf{z} = \text{vec}(\mathbf{R}) = \mathbf{B}\mathbf{p} + \sigma_n^2\mathbf{1} \quad (7)$$

where  $\mathbf{B} = [(\mathbf{A}^* \odot \mathbf{A})^T, (\mathbf{A} \odot \mathbf{A})^T, (\mathbf{A}^* \odot \mathbf{A}^*)^T]^T$  and the symbol  $\odot$  denotes the Khatri-Rao product.  $\mathbf{p} = [\sigma_1^2, \dots, \sigma_K^2]^T$ , and  $\mathbf{1} = [\bar{\mathbf{I}}^T, \bar{\mathbf{0}}^T, \bar{\mathbf{0}}^T]^T$ .  $\bar{\mathbf{I}}$  and  $\bar{\mathbf{0}}$  are the vectorization of  $\mathbf{I}$  and  $\mathbf{0}$ , respectively. It is clear that Eq. (7) can be regarded as a virtual array data model with only a single snapshot. Then, the corresponding virtual sensor positions can be expressed as

$$\mathbb{V} = \mathbb{D} \cup \mathbb{S} \cup -\mathbb{S} \quad (8)$$

where  $\mathbb{D} = \{l_i - l_j | l_i, l_j \in \mathbb{P}_1 \cup \mathbb{P}_2\}$  is the DCA. The union of  $\mathbb{S}$  and  $-\mathbb{S}$  is the SCA, where  $\mathbb{S} = \{l_i + l_j | l_i, l_j \in \mathbb{P}_1 \cup \mathbb{P}_2\}$ .  $\mathbb{V}$  denotes the SDCA.

After removing the repeated elements in  $\mathbb{V}$ , we can get the consecutive part  $\mathbb{U}$ . Then, cDOFs of  $\mathbb{V}$  is

$$\text{cDOFs} = |\mathbb{U}| \quad (9)$$

where  $\mathbb{U} \subseteq \mathbb{V}$ , and the symbol  $|\cdot|$  refers to the cardinality of a set.

Then, the virtual array output corresponding to  $\mathbb{U}$  can be formulated as

$$\mathbf{z}_0 = \mathbf{B}_0\mathbf{p} + \sigma_n^2\mathbf{1}_0 \quad (10)$$

Based on Eq. (10), spatial smoothing MUSIC (SS-MUSIC) [3] can be used to estimate the DOAs. Note that the above description is a special case for DOA estimation of noncircular signals. When the noncircular phases are not zero or the noncircular rates are less than one, the corresponding DOA estimation methods based on sparse arrays can be found in [16, 17].

### 3. PROPOSED NOVEL NESTED ARRAY FOR NONCIRCULAR SIGNALS

In this section, we first introduce the design strategy for the proposed novel nested array. Then, its properties about cDOFs and physical array aperture are analyzed. Note that, the parameter  $d$  is ignored in the remainder of this paper to simplify the analysis.

According to Eq. (1), we can give the definition of generalized TNA as follows.

**Definition 1:** Given the parameters  $N_1$  and  $N_2$ , the generalized TNA is defined as

$$\begin{cases} \mathbb{P}_1 = \{p_1 + a_1 | a_1 \in \mathbb{Q}, p_1 = 1, \dots, N_1\} \\ \mathbb{P}_2 = \{p_2(N_1 + 1) + a_2 | a_2 \in \mathbb{Q}, p_2 = 1, \dots, N_2\} \end{cases} \quad (11)$$

where  $\mathbb{Q}$  is the rational number set.

From [21], we know that TNA has the potential to increase cDOFs when its sensors are laid out properly. In addition, it can be seen from [2] that the offset configuration of two-dimensional NA can generate more virtual sensors. Accordingly, we deduce that generalized TNA may have the similar property. According to [21], we obtain the following property of generalized TNA.

**Property 1:** For generalized TNA in Definition 1, its DCA has the same form as that of NA when  $a_1 = a_2 \in \mathbb{Q}$  or  $a_1 = a_2 + (N_1 + 1)N_2 \in \mathbb{Q}$ .

The proof can be found in Appendix A. Obviously, the DCAs of generalized TNA and traditional NA are identical as long as  $a_1$  and  $a_2$  have the relationship in Property 1. Under this case, the DCA of generalized TNA can be expressed as

$$\mathbb{D} = \{-(N_1 + 1)N_2 + 1, \dots, (N_1 + 1)N_2 - 1\} \quad (12)$$

Besides, the continuous part of SCA for generalized TNA can be denoted as

$$\begin{cases} \mathbb{U}_{\text{SCA}}^1 = \mathbb{U}_1 \cup -\mathbb{U}_1, & \text{if } a_1 = a_2 \in \mathbb{Q} \\ \mathbb{U}_{\text{SCA}}^2 = \mathbb{U}_2 \cup -\mathbb{U}_2, & \text{if } a_1 = a_2 + (N_1 + 1)N_2 \in \mathbb{Q} \end{cases} \quad (13)$$

where  $\mathbb{U}_1 = \{2 + 2a_2, \dots, M + 2a_2\}$ ,  $\mathbb{U}_2 = \{M + 2a_2, \dots, 2M - 2 + 2a_2\}$ , and  $M = (N_1 + 1)(N_2 + 1)$ . It is clear from Eq. (13) that the SCA can be utilized to improve the underdetermined DOA estimation performance of noncircular signals.

From Eq. (8), we know that SDCA is the union of DCA and SCA. Some repeated elements between DCA and SCA always exist for the presented sparse arrays [15, 17, 19, 20], which will decrease the available cDOFs. Fig. 1 provides an example of NADiS to illustrate this phenomenon, where the number of physical sensors is fixed to be 5. The physical sensor positions are specified as  $\{0, 1, 2, 7, 12\}$ . The DCA and SCA can be respectively denoted as  $\mathbb{D} = \{0, \pm 1, \pm 2, \pm 5, \pm 6, \pm 7, \pm 10, \pm 11, \pm 12\}$  and  $\mathbb{S} = \{0, \pm 1, \pm 2 \pm 3, \pm 4, \pm 7, \pm 8, \pm 9, \pm 12, \pm 13, \pm 14, \pm 19, \pm 24\}$ . Obviously, we can find that the repeated elements between  $\mathbb{D}$  and  $\mathbb{S}$  are  $\{0, \pm 1, \pm 2, \pm 7, \pm 12\}$ . In addition, it is obvious that the SDCA of NADiS is discontinuous. From the above analysis, we know that the cDOFs may increase significantly after the corresponding discontinuous parts of SDCA and the repeated elements between DCA and SCA are eliminated.

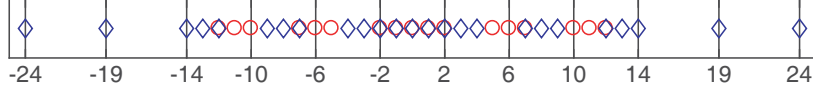


**Figure 1.** The DCA and SCA of NADiS with 5 physical sensors, where red circles and blue rhombuses denotes the elements in DCA and SCA, respectively.

Reviewing the offset configuration of two-dimensional NA [2], we can find that the cross-difference result between the dense subarray and sparse subarray is essentially the cross-sum. Obviously, its virtual array is the union of DCA and SCA in nature, i.e., SDCA. Compared with sensor configurations I and II in [2], the offset configuration can not only generate the continuous SDCA, but also can achieve the largest cDOFs. Inspired by this finding, we obtain the following property.

**Property 2:** When  $a_1 = a_2 = -(N_1 + 1)(2N_2 + 1)/2$ , or  $a_1 = (N_1 + 1)(2N_2 - 1)/2$  and  $a_2 = -(N_1 + 1)/2$ , the generalized TNA can generate the continuous SDCA with the maximum cDOFs, i.e.,  $\text{cDOFs} = 2(N_1 + 1)(2N_2 + 1) - 3$ .

The proof of Property 2 is omitted here since it has a similar process to that described in Appendix B of [21]. From Property 2, we know that there are two different cases for  $a_1$  and  $a_2$  to achieve the same and maximum cDOFs. That is to say, there are no repeated elements between DCA and SCA. For the first case, i.e.,  $a_1 = a_2 = -(N_1 + 1)(2N_2 + 1)/2$ , the specific expressions of generalized TNA can be denoted as

$$\begin{cases} \mathbb{P}_{\text{S1},1} = \{p_1 - (N_1 + 1)(2N_2 + 1)/2 | p_1 = 1, \dots, N_1\} \\ \mathbb{P}_{\text{S1},2} = \{(p_2 - (2N_2 + 1)/2)(N_1 + 1) | p_2 = 1, \dots, N_2\} \end{cases} \quad (14)$$

While for the second case, i.e.,  $a_1 = (N_1 + 1)(2N_2 - 1)/2$  and  $a_2 = -(N_1 + 1)/2$ , the specific expressions

of generalized TNA can be modified as

$$\begin{cases} \mathbb{P}_{S2,1} = \{p_1 - N_1 - 1 + (N_1 + 1)(2N_2 + 1)/2 | p_1 = 1, \dots, N_1\} \\ \mathbb{P}_{S2,2} = \{(p_2 - N_2 - 1 + (2N_2 + 1)/2)(N_1 + 1) | p_2 = 1, \dots, N_2\} \end{cases} \quad (15)$$

Observing Eqs. (14) and (15), we can find that  $\mathbb{P}_{S1,1} = -\mathbb{P}_{S2,1}$  and  $\mathbb{P}_{S1,2} = -\mathbb{P}_{S2,2}$ . Then, it is easy to know that the generalized TNAs under this two cases are mirror symmetric about zero point. Based on the above analysis, the proposed novel nested configuration can be defined as follows.

**Definition 2:** Given parameters  $N_1$  and  $N_2$ , the proposed novel nested array can be defined as

$$\begin{cases} \mathbb{P}_1 = f\{p_1 + (N_1 + 1)(2N_2 - 1)/2 | p_1 = 1, \dots, N_1\} \\ \mathbb{P}_2 = f\{p_2(N_1 + 1) - (N_1 + 1)/2 | p_2 = 1, \dots, N_2\} \end{cases} \quad (16)$$

where the operation  $f\{\cdot\}$  is defined as  $f\{x_1, x_2, x_3, x_4, \dots\} = \{x_1, -x_2, x_3, -x_4, \dots\}$ .

From Definition 2, we can easily determine the physical array aperture as

$$L_{PA} = (N_1 + 1)(2N_2 + 1) - 3 \quad (17)$$

To achieve the maximum cDOFs for the fixed physical sensor number, we need to solve the following optimization equation:

$$\begin{aligned} & \max_{N_1, N_2 \in \mathbb{Z}^+} 2(N_1 + 1)(2N_2 + 1) - 3 \\ & \text{subject to: } N_1 + N_2 = N \end{aligned} \quad (18)$$

It is easy from Eq. (18) to know that the optimal solutions are

$$\begin{cases} N_1 = (N - 1)/2, N_2 = (N + 1)/2, & N \text{ is odd} \\ N_1 = N_2 = N/2, & N \text{ is even} \end{cases} \quad (19)$$

According to Eq. (19), we can obtain the corresponding expressions of cDOFs and physical array aperture as

$$\text{cDOFs} = N^2 + 3N - 1 \quad (20)$$

$$L_{PA} = (N^2 + 3N - 4)/2 \quad (21)$$

An example is shown in Fig. 2, where  $N = 8$ . From Eq. (19), we can determine that  $N_1 = N_2 = 4$ . Then, the physical sensor position sets of the proposed array are  $\mathbb{P}_1 = \{18.5, -19.5, 20.5, -21.5\}$ , and  $\mathbb{P}_2 = \{2.5, -7.5, 12.5, -17.5\}$ . It can be seen from Fig. 2(a) that the physical array aperture of proposed array is equal to 42. Fig. 2(b) gives the corresponding virtual array, which is continuous. More importantly, the union of DCA and SCA does not have repeated elements, which can help to increase the cDOFs. From Fig. 2(b), we know that the number of cDOFs is equal to 87. The above results is in accordance with Eqs. (16), (19)–(21).

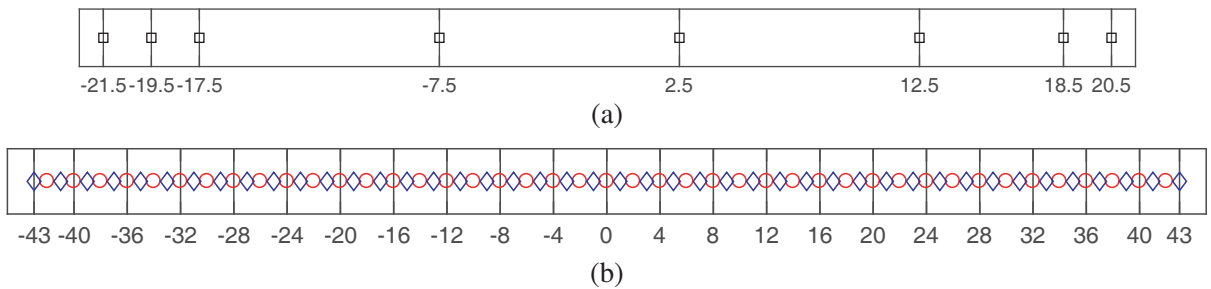


**Figure 2.** An example of the proposed novel nested array with 8 physical sensors. (a) Physical sensors distribution of the proposed array, where  $\mathbb{P}_1 = \{18.5, -19.5, 20.5, -21.5\}$ ,  $\mathbb{P}_2 = \{2.5, -7.5, 12.5, -17.5\}$ . (b) The corresponding virtual array, which is the union of DCA and SCA. Black squares represent the physical sensors.

## 4. SIMULATION RESULTS

In this section, we select NNA [15], DsCAMpS [17], NADiS [19], and SANC [20] as the comparison arrays. To demonstrate the superiority of the proposed array, cDOFs and physical array aperture of the proposed array are first studied. Then, normalized spectrum of the proposed array is provided to verify the DOA estimation validity. In the end, we give the root-mean-squared error (RMSE) results to evaluate the DOA estimation performance of the proposed array for noncircular signals. It should be noted that the unit inter-element spacing is set as half a wavelength in the following experiments.

### 4.1. cDOFs and Physical Array Aperture

In the first experiment, we study the cDOFs and physical array aperture of the proposed array. Let the total physical sensor number  $N$  vary from 2 to 30. According to the definitions of NNA, DsCAMpS, NADiS, and the proposed array, we can determine their specific sensor position sets respectively. Note that SANC is obtained by exhaustion method. Hence, its configurations are provided under the condition of  $2 \leq N \leq 10$ .

Figure 3(a) shows the comparisons about cDOFs, while Fig. 3(b) depicts the curves about physical array aperture. It can be seen from Fig. 3 that the proposed array possesses larger cDOFs and physical array aperture than the other comparison arrays. Thus, the proposed array can identify more noncircular signals and owns better estimation performance in comparison with NNA, DsCAMpS, NADiS, and SANC.

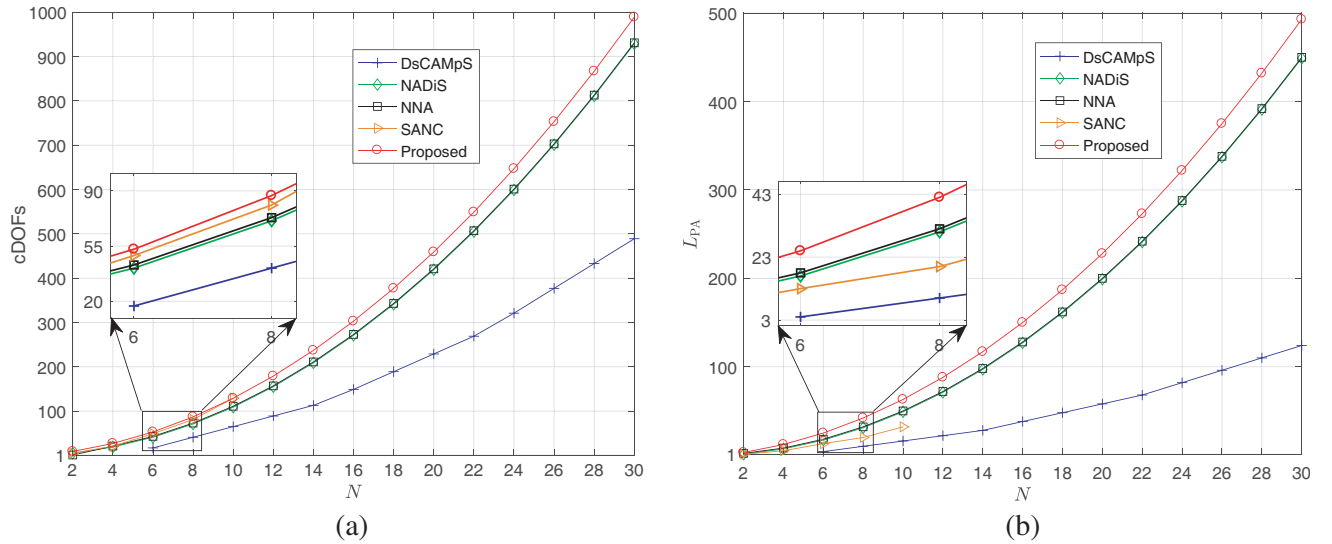


**Figure 3.** Comparisons of (a) cDOFs, (b) physical array aperture.

### 4.2. Normalized Spectrum

In the second experiment,  $N$  is fixed to be 8 to show the DOA estimation effectiveness of the proposed array. According to Fig. 2(a), we know that the physical sensor positions of the proposed array are  $\{-21.5, -19.5, -17.5, -7.5, 2.5, 12.5, 18.5, 20.5\}$ . Consider that  $K = 41$  BPSK signals with uniform distribution between  $-60^\circ$  and  $60^\circ$  impinge on this array. Both SNR and snapshots are considered ideal, i.e., the array output data is noiseless and possesses infinite number of snapshots. Then, SS-MUSIC with  $0.01^\circ$  search interval is used to estimate the DOAs.

As shown in Fig. 4 is the normalized spectrum. Obviously, the DOAs of all BPSK signals are estimated correctly, which verifies the validity of the proposed array.

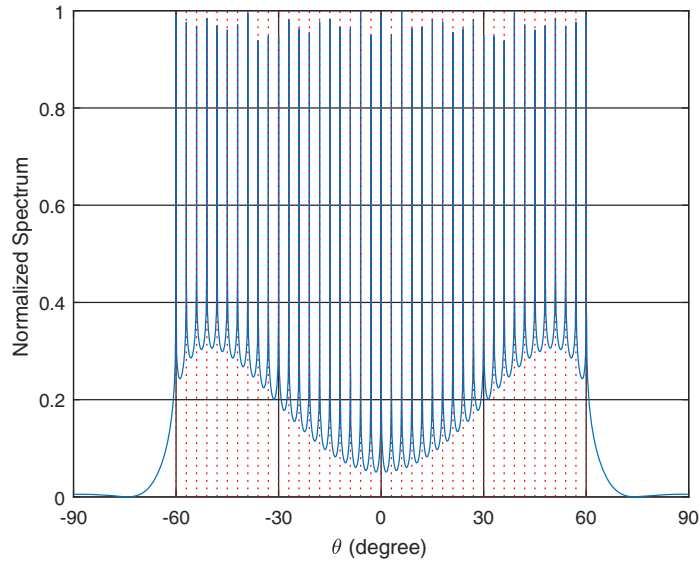


Figure 4. Normalized spectrum of the proposed array, where  $N = 8$ , and  $K = 41$ .

### 4.3. RMSE

To further evaluate the DOA estimation performance of the proposed array, RMSE experiments are conducted in this subsection. Similar to the previous subsection,  $N$  is set to 8. Then, the sensor positions of NNA, DsCAMpS, NADiS, and SANC can be respectively given as  $\{0, 1, 2, 3, 11, 18, 25, 32\}$ ,  $\{0, 2, 3, 4, 6, 8, 9, 10\}$ ,  $\{0, 1, 2, 3, 4, 13, 22, 31\}$ , and  $\{0, 6, 12, 15, 16, 17, 19, 20\}$ . The sensor positions of the proposed array are the same as that in the previous subsection. Thus, the cDOFs of the above five sparse arrays are 73, 41, 71, 81, and 87, respectively. In addition, the corresponding physical array apertures can be respectively given as 32, 10, 31, 20, and 42. Assume that there are  $K = 15$  BPSK signals with uniform distribution between  $-60^\circ$  and  $60^\circ$  impinging on the above arrays. The DOA estimation method and search interval keep unchanged compared with the previous experiment. Then, we can know that the number of identifiable noncircular signals for NNA, DsCAMpS, NADiS, SANC,

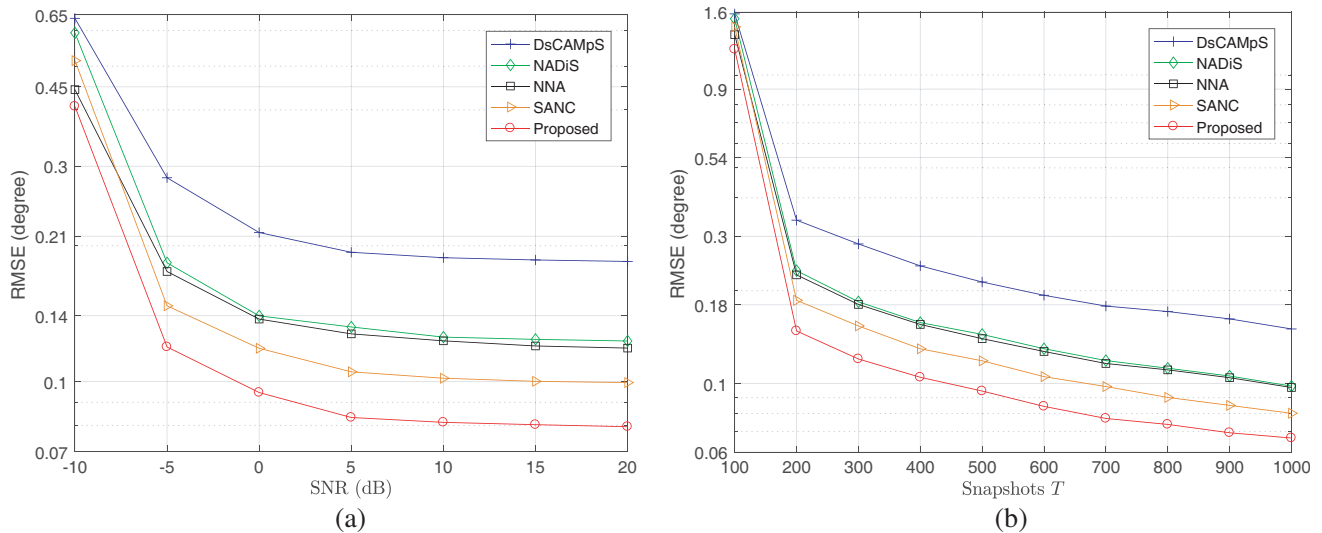


Figure 5. RMSE results for five different sparse arrays, where  $N = 8$ ,  $K = 15$ . (a) RMSE versus SNR, where  $T = 500$ , (b) RMSE versus snapshots, where SNR = 0 dB.

and the proposed array are 36, 20, 35, 40, and 43, respectively. The RMSE results are calculated according to the following expression:

$$\text{RMSE} = \sqrt{\frac{1}{IK} \sum_{i=1}^I \sum_{k=1}^K (\hat{\theta}_k(i) - \theta_k)^2} \quad (22)$$

where  $I = 500$  is the number of Monte Carlo trials, and  $\hat{\theta}_k(i)$  is the estimated DOA of  $\theta_k$  in the  $i$ th trial.

Figure 5(a) shows the RMSE curves as a function of SNR, where the number of snapshots is fixed as 500. Fig. 5(b) is the RMSE results versus snapshots under the condition of SNR = 0 dB. It can be observed from Fig. 5 that the RMSE curves of all sparse arrays decrease as the increase of SNR and snapshots. Moreover, the proposed array always possesses less RMSE than the other four arrays, especially in the case of high SNR and snapshots. The reason is that the cDOFs and physical array aperture of the proposed array are larger than those of NNA, DsCAMpS, NADiS, and SANC. Thus, we can conclude that our proposed array possesses the best DOA estimation performance among all the five sparse arrays.

## 5. CONCLUSION

In this paper, we have proposed a novel nested array for DOA estimation of noncircular signals. Before giving this novel sparse array, we first introduce the generalized TNA concept. Then, the relationship between DCA and SCA is investigated. By using the properties of generalized TNA, we finally construct the proposed array configuration. In addition, the optimal selections of  $N_1$  and  $N_2$  are also provided so as to achieve the maximum cDOFs and the largest physical aperture. Finally, simulation results demonstrate the superiority of the proposed array for the DOA estimation of noncircular signals.

## APPENDIX A. PROOF OF PROPERTY 1

From [8, 21], we know that the DCA of a sparse array can be expressed as the union of its self-difference and cross-difference. Thus, the DCA of the generalized TNA can be expressed as

$$\mathbb{D} = (\mathbb{P}_1 - \mathbb{P}_1) \cup (\mathbb{P}_2 - \mathbb{P}_2) \cup (\mathbb{P}_1 - \mathbb{P}_2) \cup (\mathbb{P}_2 - \mathbb{P}_1) \quad (A1)$$

where  $\mathbb{P}_1 = \{p_1 + a_1 | a_1 \in \mathbb{Q}, p_1 = 1, \dots, N_1\}$  and  $\mathbb{P}_2 = \{p_2(N_1 + 1) + a_2 | a_2 \in \mathbb{Q}, p_2 = 1, \dots, N_2\}$ . Then, we have

$$\mathbb{P}_1 - \mathbb{P}_1 = \{-N_1 + 1, -N_1 + 2, \dots, N_1 - 2, N_1 - 1\} \quad (A2)$$

$$\mathbb{P}_2 - \mathbb{P}_2 = \{-(N_2 - 1)(N_1 + 1), -(N_2 - 2)(N_1 + 1), \dots, (N_2 - 2)(N_1 + 1), (N_2 - 1)(N_1 + 1)\} \quad (A3)$$

$$\mathbb{P}_2 - \mathbb{P}_1 = \{p_2(N_1 + 1) - p_1 + a_2 - a_1 | a_1, a_2 \in \mathbb{Q}, p_1 = 1, \dots, N_1, p_2 = 1, \dots, N_2\} \quad (A4)$$

In addition, it is obvious from Eq. (A1) that  $\mathbb{P}_1 - \mathbb{P}_2$  and  $\mathbb{P}_2 - \mathbb{P}_1$  are mirror symmetric about zero point. Observing Eq. (11), we can find that the generalized TNA will become the traditional NA when  $a_1 = a_2 = 0$ . Accordingly, the DCA of NA can be expressed as

$$\mathbb{D}_{\text{NA}} = (\mathbb{P}_1 - \mathbb{P}_1) \cup (\mathbb{P}_2 - \mathbb{P}_2) \cup (\mathbb{P}_{1,0} - \mathbb{P}_{2,0}) \cup (\mathbb{P}_{2,0} - \mathbb{P}_{1,0}) \quad (A5)$$

where  $\mathbb{P}_{2,0} - \mathbb{P}_{1,0} = -(\mathbb{P}_{1,0} - \mathbb{P}_{2,0}) = \{p_2(N_1 + 1) - p_1 | p_1 = 1, \dots, N_1, p_2 = 1, \dots, N_2\}$ . For convenience of analysis, let  $\mathbb{U}_{p_2} = \{p_2(N_1 + 1) - p_1 | p_1 = 1, \dots, N_1\}$ . It is apparent that  $\mathbb{U}_{p_2}$  is fully continuous and possesses  $N_1$  elements. Then, the cross-difference existing in Eq. (A5) can be denoted as

$$(\mathbb{P}_{1,0} - \mathbb{P}_{2,0}) \cup (\mathbb{P}_{2,0} - \mathbb{P}_{1,0}) = -\mathbb{U}_{N_2} \cup -\mathbb{U}_{N_2-1} \cup \dots \cup \mathbb{U}_{N_2-1} \cup \mathbb{U}_{N_2} \quad (A6)$$

Combining Eqs. (A1) and (A5), we can deduce that when the DCA of generalized TNA has the same form as that of NA,  $(\mathbb{P}_1 - \mathbb{P}_2) \cup (\mathbb{P}_2 - \mathbb{P}_1) = (\mathbb{P}_{1,0} - \mathbb{P}_{2,0}) \cup (\mathbb{P}_{2,0} - \mathbb{P}_{1,0})$  should hold true. Next, let  $\tilde{\mathbb{U}}_{p_2} = \{p_2(N_1 + 1) - p_1 + a_2 - a_1 | a_1, a_2 \in \mathbb{Q}, p_1 = 1, \dots, N_1\}$  denote a continuous part of  $\mathbb{P}_2 - \mathbb{P}_1$ . Then, the cross-difference in the DCA of generalized TNA can be expressed as

$$(\mathbb{P}_1 - \mathbb{P}_2) \cup (\mathbb{P}_2 - \mathbb{P}_1) = -\tilde{\mathbb{U}}_{N_2} \cup -\tilde{\mathbb{U}}_{N_2-1} \cup \dots \cup \tilde{\mathbb{U}}_{N_2-1} \cup \tilde{\mathbb{U}}_{N_2} \quad (A7)$$

Obviously, there are two different cases for  $\tilde{U}_{p_2, p_2} = 1, \dots, N_2$  to make  $(\mathbb{P}_1 - \mathbb{P}_2) \cup (\mathbb{P}_2 - \mathbb{P}_1) = (\mathbb{P}_{1,0} - \mathbb{P}_{2,0}) \cup (\mathbb{P}_{2,0} - \mathbb{P}_{1,0})$  hold.

For the first case, i.e.,  $\tilde{U}_{p_2} \geq 0$ , where  $p_2 = 1, \dots, N_2$ , it is obvious that  $\tilde{U}_{p_2} = U_{p_2}$  with  $p_2 = 1, \dots, N_2$  should hold true. Then, we can easily get that  $a_2 - a_1 = 0$ , which means  $a_2 = a_1 \in \mathbb{Q}$ .

For the second case, i.e.,  $\tilde{U}_{p_2} < 0$ , where  $p_2 = 1, \dots, N_2$ , according to the definition of  $U_{p_2}$ , we know that  $U_{p_2} > 0$  with  $p_2 = 1, \dots, N_2$  always holds true. In this case, we can prove  $\tilde{U}_{p_2} = -U_{N_2+1-p_2}$  for  $p_2 = 1, \dots, N_2$  hold true. Then, we can easily get that  $a_1 = a_2 + (N_1 + 1)N_2 \in \mathbb{Q}$ . The above is the proof of Property 1.

## ACKNOWLEDGMENT

This work was supported in part by the the National Natural Science Foundation of China under Grant 61671168 and Grant 61801143, in part by the National Natural Science Foundation of Heilongjiang Province under Grant LH2019F010, and in part by the Fundamental Research Funds for the Central Universities under Grant 3072019CF0801 and Grant 3072019CFM0802.

## REFERENCES

1. Pal, P. and P. Vaidyanathan, "Nested arrays: A novel approach to array processing with enhanced degrees of freedom," *IEEE Trans. Signal Process.*, Vol. 58, No. 8, 4167–4181, Aug. 2010.
2. Pal, P. and P. Vaidyanathan, "Nested arrays in two dimensions, Part I: Geometrical considerations," *IEEE Trans. Signal Process.*, Vol. 60, No. 9, 4694–4705, Sep. 2012.
3. Pal, P. and P. P. Vaidyanathan, "Coprime sampling and the MUSIC algorithm," *Proc. 14th IEEE DSP/SPE Workshop*, 289–294, Sedona, AZ, USA, Jan. 2011.
4. Zhou, C., Y. Gu, X. Fan, Z. Shi, G. Mao, and Y. D. Zhang, "Direction-of-arrival estimation for coprime array via virtual array interpolation," *IEEE Trans. Signal Process.*, Vol. 66, No. 22, 5956–5971, Nov. 2018.
5. Liu, S., Q. Liu, J. Zhao, and Z. Yuan, "Triple two-level nested array with improved degrees of freedom," *Progress In Electromagnetics Research*, Vol. 84, 135–151, 2019.
6. Moffet, A., "Minimum-redundancy linear arrays," *IEEE Trans. Antennas Propag.*, Vol. 16, No. 2, 172–175, Mar. 1968.
7. Vaidyanathan, P. P. and P. Pal, "Sparse sensing with co-prime samplers and arrays," *IEEE Trans. Signal Process.*, Vol. 59, No. 2, 573–586, Feb. 2011.
8. Qin, S., Y. D. Zhang, and M. G. Amin, "Generalized coprime array configurations for direction-of-arrival estimation," *IEEE Trans. Signal Process.*, Vol. 63, No. 6, 1377–1390, Mar. 2015.
9. Shi, J., G. Hu, X. Zhang, and H. Zhou, "Generalized nested array: Optimization for degrees of freedom and mutual coupling," *IEEE Commun. Lett.*, Vol. 22, No. 6, 1208–1211, Jun. 2018.
10. Zheng, Z., W.-Q. Wang, Y. Kong, and Y. D. Zhang, "MISC array: A new sparse array design achieving increased degrees of freedom and reduced mutual coupling effect," *IEEE Trans. Signal Process.*, Vol. 67, No. 7, 1728–1741, Apr. 2019.
11. Chargé, P., Y. Wang, and J. Saillard, "A non-circular sources direction finding method using polynomial rooting," *Signal Process.*, Vol. 81, No. 8, 1765–1770, Jul. 2001.
12. Zoubir, A., P. Chargé, and Y. Wang, "Non circular sources localization with ESPRIT," *Proc. European Conference on Wireless Technology (ECWT)*, Munich, Germany, Oct. 2003.
13. Abeida, H. and J.-P. Delmas, "MUSIC-like estimation of direction of arrival for noncircular sources," *IEEE Trans. Signal Process.*, Vol. 54, No. 7, 2678–2690, Jun. 2006.
14. Zhai, H., X. Zhang, W. Zheng, and P. Gong, "DOA estimation of noncircular signals for unfolded coprime linear array: Identifiability, DOF and algorithm (May 2018)," *IEEE Access*, Vol. 6, 29382–29390, May 2018.

15. Iwazaki, S. and K. Ichige, "Underdetermined direction of arrival estimation by sum and difference composite co-array," *2018 25th IEEE International Conference on Electronics, Circuits and Systems (ICECS)*, 669–672, Bordeaux, France, Dec. 2018.
16. Cai, J., W. Liu, R. Zong, and B. Wu, "Sparse array extension for non-circular signals with subspace and compressive sensing based DOA estimation methods," *Signal Process.*, Vol. 145, 59–67, Apr. 2018.
17. Chen, Z., Y. Ding, S. Ren, and Z. Chen, "A novel noncircular MUSIC algorithm based on the concept of the difference and sum coarray," *Sensors*, Vol. 18, No. 2, 344–360, 2018.
18. Cai, J., B. Wu, P. Li, and W. Liu, "A sparse representation based DOA estimation algorithm for a mixture of circular and noncircular signals using sparse arrays," *Proc. IEEE Int. Conf. Commun.*, 1–5, Paris, France, May 2017.
19. Gupta, P. and M. Agrawal, "Design and analysis of the sparse array for DOA estimation of noncircular signals," *IEEE Trans. Signal Process.*, Vol. 67, No. 2, 460–473, Jan. 2018.
20. Zhang, Y.-K., H.-Y. Xu, D.-M. Wang, B. Ba, and S.-Y. Li, "A novel designed sparse array for noncircular sources with high degree of freedom," *Math. Problems Eng.*, Vol. 2019, Art. No. 1264715, 2019.
21. Si, W., Z. Peng, C. Hou, and F. Zeng, "Improved nested arrays with sum-difference coarray for DOA estimation," *IEEE Sensors J.*, Vol. 19, No. 16, 6986–6997, Apr. 2019.